Persistent photoconductivity at elevated temperatures in $Cd_{1-x}Mn_xTe:In$

C. Leighton and I. Terry
Department of Physics, Science Laboratories, University of Durham, South Road, Durham, DH1 3LE, England

P. Becla
Department of Materials Science and Engineering, Massachusetts Institute of Technology, Cambridge, Massachusetts 02139
(Received 23 December 1996)

Persistent photoconductivity measurements have been made on several samples of $Cd_{1-x}Mn_xTe:In$ with manganese concentrations in the range 5–15 %. The effect of composition on the persistent photoconductivity (PPC) effect has been studied. The PPC is usually quenched at a temperature of about 100 K but some samples exhibit PPC which exists up to 190 K. The origin of this effect is discussed in terms of several models of PPC. Particular attention is paid to the various possibilities for multiple *DX*-like centers in these materials. Also, a small number of samples have been identified as being possible candidates for being driven through the insulator-metal transition via photodoping. One possible application of these samples (which has already been suggested) would be to write erasable conductive, or even metallic, patterns on an insulating background. The requirements for this area of application are discussed in order to ascertain whether $Cd_{1-x}Mn_xTe:In$ is a suitable material. [S0163-1829(97)04235-5]

I. INTRODUCTION

Persistent photoconductivity (PPC) was discovered in $Cd_{1-x}Mn_xTe$ (see Ref. 1 and the references within) following work on the effect in the II-VI semiconductors $Cd_{1-x}Zn_xTe$ (Refs. 2 and 3) and CdTe (under hydrostatic pressure),[4] when doped with presumably substitutional donors. It has since been demonstrated that the donors in these compounds behave in a manner analogous to that of the *DX* center in $Al_xGa_{1-x}As$.[5] Furthermore, it is widely accepted that the model of the *DX* center due to Chadi and Chang[6,7] is consistent with the PPC effect in these II-VI and III-V alloys.

One immediate application of the PPC in these materials has been to write erasable conductive patterns on an insulating background, as demonstrated in $Al_xGa_{1-x}As$ epilayers.[8,9] This process could be utilized in optical switching, holography, and high-density data storage if the following requirements are met: room-temperature PPC, and high differences in conductivity between illuminated (conductive) and unilluminated (insulating) regions. It has also been noted[9] that, as optical diffraction from conductivity gratings (formed from patterns of illuminated regions) increases with the square of the grating thickness, bulk samples are preferable for such applications.

It has been suggested that II-VI semiconductors show promise of supporting *DX* centers with larger capture barriers, resulting in higher PPC quenching temperatures. Thio *et al.* have shown that $Cd_{0.72}Zn_{0.28}Te:Cl$ could be a suitable material, with the PPC existing up to 190 K.[10] This high quenching temperature was attributed to a second *DX*-like center as predicted by the first-principles pseudopotential calculations of Park and Chadi.[11] Here the large lattice relaxation negative *U* model is used to calculate the binding energies of the *DX* centers due to group-III and group-VII donors in CdTe, ZnTe, and $Cd_{1-x}Zn_xTe$. The calculations suggest that for group-VII doping there are *three* types of large lattice relaxations possible, each having a different structure to the original ''broken bond'' *DX* state. Obviously these structures have different binding energies which can explain why they will support PPC to different temperatures. An interesting point which emerges from their calculation is that the situation for group-III donors such as In is rather different—only one *DX*-like state is possible.

One problem with $Cd_{0.72}Zn_{0.28}Te:Cl$ could be the fact that the samples reported so far appear to be on the insulating side of the metal-insulator transition (MIT) even after illumination. Bennett *et al.*[12] claim to have demonstrated a transition from insulating to metallic behavior by observing a superlinear exposure dependence of the carrier density at 50 K. However, Katsumoto[13] has made a complete study of the MIT by continuously varying the photodoping level in $Al_xGa_{1-x}As$ at low temperatures, and has found a linear variation of carrier density on illumination exposure in going through the phase transition. In fact, the work by Thio *et al.*,[8] which undoubtedly involves conductive patterns in $Al_xGa_{1-x}As$ that are metallic, also demonstrates a linear dependence of carrier density upon light exposure.

In this paper it is proposed that $Cd_{1-x}Mn_xTe:In$ is another attractive choice for a material where conductivity gratings may be produced by PPC. It is demonstrated that it may be possible to photodope the material through the metal-insulator transition, and that, under suitable conditions, persistent photoconductivity may be observed up to a temperature of 190 K. This high temperature PPC appears to arise from at least two *DX*-like centers associated with the indium donor which is in apparent disagreement with the conclusions of Park and Chadi[11] on the nature of group-III donors in II-VI semiconductors. Possible origins of the high-temperature PPC in $Cd_{1-x}Mn_xTe:In$ are discussed.

The structure of this paper is as follows. Section II describes the samples used in this study, while Sec. III describes the experimental procedure for the PPC experiments. Results of the experiments and a discussion of them are pre-

TABLE I. Phototransport data for sample set A. The quantities listed are the nominal Mn concentration (x), the resistivity (ρ) at 300 K/4.2 K, the deep level activation energy (E_D), the PPC quenching temperature (T_Q), the change in resistivity on illumination (ρ_L-ρ_D)/ρ_L, the carrier concentration (n), and the mobility (μ) at 300 K. N/A denotes a value that is not available. * denotes determination by mass spectroscopy.

Sample No.	Nominal x	ρ (300 K) (Ω cm)	ρ (4.2 K) (Ω cm)	E_D (mev)	T_Q (K)	$\Delta\rho_{\rm ill}/\rho_L$	n (300 K) (cm^{-3})	μ (300 K) ($\mathrm{cm}^{-2}\ \mathrm{V}\ \mathrm{s}^{-1}$)	Annealing Temp. (°C)	EDAX x (%)
A1	0.05	0.052	0.126	5.44	91.1	23.8%	1.4×10^{17}	858	800	
A2	0.075	0.150	2.844	14.84	96.6	67.1%	1.1×10^{17}	373	600	6.43*
A3	0.10	0.055	5.339	18.64	104.4	87.5%	2.0×10^{17}	568	800	8.10 ± 0.2
A4	0.15	11.65	N/A	162.5	121.0	N/A	2.6×10^{15}	208	600	14.8 ± 0.3

sented in Sec. IV. The work is summarized and conclusions are drawn in Sec. V.

II. SAMPLES

The vertical Bridgman growth technique was employed to produce bulk single crystals of $Cd_{1-x}Mn_xTe$ doped with indium. The crystals were then annealed in a cadmium atmosphere in order to reduce the level of compensation in the material due to cadmium vacancies. This study is concerned with two sets of samples (A and B) as summarized in Tables I and II. Here the x values are determined from energy dispersive analysis of x-rays (EDAX).

Set A contains four samples with concentrations nominally 5%, 7.5%, 10%, and 15% Mn. Growing crystals with Mn concentrations greater than this results in samples so insulating that electrical transport measurements become rather difficult.

Set B consists of five samples all cut from the same crystal. Each of the samples was taken from a cross-sectional slice through the crystal made at various distances along the crystal from one end. Although the whole crystal was grown to be nominally 10% Mn, a concentration gradient existed along the crystal meaning that each slice had a slightly different Mn concentration. These cross-sectional slices were cut with increasing thickness from 380 up to 1340 μm.

III. EXPERIMENTAL PROCEDURE

The samples were prepared for electrical measurements by etching in a 3% Br (by volume) in CH_3OH solution. Ohmic contacts were made by indium soldering 50-μm diameter gold wires on to the etched surface of the sample in a Van der Pauw configuration. The samples were mounted on sapphire wafers using a small amount of high-thermal-conductivity varnish. The sapphire wafers were then attached to a copper sample holder placed in a variable-temperature continuous flow cryostat, which is situated between the pole pieces of an electromagnet capable of magnetic fields up to 0.75 T. Resistivity and Hall-effect measurements were then made as a function of temperature from 360 to 4.2 K using standard dc techniques. Some resistivity measurements were also made by direct immersion in liquid helium. The system allows measurements of resistance in the range 1 mΩ up to 300 MΩ.

The phototransport measurements were performed with illumination by subband-gap radiation, the band gap of $C_{0.9}Mn_{0.1}Te$:In being 1.754 eV at 4.2 K. This was done using an infrared GaAs light emitting diode (LED), the emission of these devices peaking at 940 nm (i.e., 1.323 eV). The LED is wired in series with a 300 Ω resistor to allow the current flowing in the LED, and hence the light intensity to be varied by varying the applied voltage.

IV. RESULTS AND DISCUSSIONS

The electrical transport data for sample set A is summarized in Table I. The temperature dependence of the resistivity of a typical sample (A3) is shown in Fig. 1, where measurements were made in the region from 4.2 K up to room temperature at various illumination levels. In each case illumination took place with the sample and LED immersed in liquid helium. In the figure the curves are labeled with the Hall free-carrier concentration at an arbitrary temperature of 16.5 K. Figure 2 shows both the resistivity and the Hall mobility as a function of the free-carrier concentration, n, again at 16.5 K. As can be seen from Figs. 1 and 2 the free-carrier concentration in this sample can be varied from 8.34×10^{16} cm^{-3} up to 2.83×10^{17} cm^{-3} by photodoping. For the sake of comparison these values for the $\sim$5% sample (A1), which has the highest conductivity of all the

TABLE II. Phototransport data for sample set B. The quantities listed are the thickness of the sample, the 300-K resistivity (ρ), carrier concentration (n), and mobility (μ), and the PPC quenching temperature (T_Q).

Sample No.	Thickness (μm)	ρ (300 K) (Ω cm)	n (300 K) (cm^{-3})	μ (300 K) ($\mathrm{cm}^2\ \mathrm{V}^{-1}\ \mathrm{s}^{-1}$)	T_Q (K)	Annealing Temperature (°C)	EDAX x (%)
B4	380	4.03	6.4×10^{15}	242	180	800	10.0 ± 0.6
B5	660	0.41	6.7×10^{16}	227	109	800	10.0 ± 0.4
B6	730	1.34	1.6×10^{16}	299	125	800	12.9 ± 0.3
B7	1340	2.19	3.7×10^{16}	78	108	800	9.07 ± 0.3
B8	1340	4.85	6.4×10^{15}	203	115	800	14.2 ± 0.3

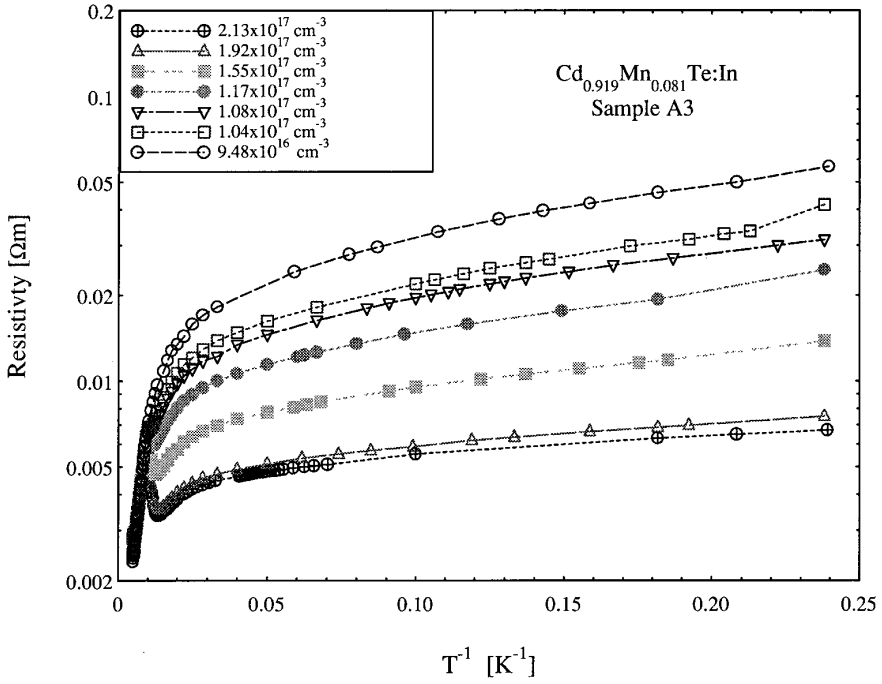

FIG. 1. Resistivity of sample A3 (8.1% Mn) as a function of inverse temperature, from room temperature to 4.2 K. Dark data and data for six photogenerated carrier concentrations are shown. The curves are labeled with the carrier concentrations measured at 16.5 K.

samples in this study, are 1.2×10^{17} and 1.63×10^{17} cm^{-3}.

It is interesting to compare these values of resistivity and carrier concentration with the Mott minimum metallic conductivity ($\sigma_{\min}$) and the MIT critical carrier concentration (n_c),[14] as given by

$$\sigma_{\min}\approx\frac{Ce^2}{\hbar a},\quad n_c\approx\left(\frac{0.26}{a_H}\right)^3,$$

where $C\sim0.03$, a is the distance between electrons ($\sim n^{-1/3}$), and a_H is the effective Bohr radius of the donor. a_H is readily estimated for CdTe by using the hydrogenic theory of shallow donors with an effective mass, $m^*=0.096m_e$ and a relative permittivity, $\varepsilon=9.7$, giving a critical carrier concentration of $n_c\sim1.1\times10^{17}$ cm^{-3}, and a minimum metallic conductivity of $\sigma_{\min}\sim5(\Omega\,\mathrm{cm})^{-1}$. So the value of carrier concentration and resistivity for the 5% and 10% samples is rather close to the ones at which an insulator-metal transition will occur. Hence, there is a strong possibility that an insulator-metal transition in $Cd_{1-x}Mn_x$Te:In could be studied by photodoping as well as the application of a magnetic field.[15,16] It is noted however that the critical carrier concentration for $Cd_{1-x}Mn_x$Te:In will be higher than that for CdTe. Shapira *et al.*[17] found that n_c increased with x and suggested that $n_c\sim2\times10^{-17}$ cm^{-3} for $x=0.05$. In a similar study on $Cd_{1-x}Mn_x$Se (Ref. 18) they found again that the critical carrier concentration increases with increasing x. This increase in critical carrier concentration with x for alloys of the form $A_{1-x}Mn_xB$ is partially due to the fact that increasing x raises the level of alloy disorder in the system [this is also demonstrated by the increase in n_c of Al_xGa_{1-x}As over the value expected for GaAs (Refs. 13,19)]. Even in the absence of disorder one

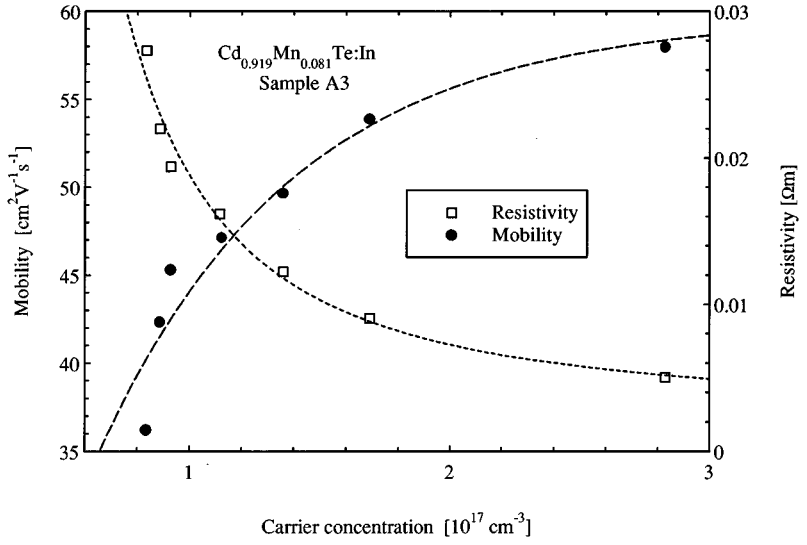

FIG. 2. The resistivity and Hall mobility of sample A3 (8.1% Mn) against the Hall carrier concentration at 16.5 K. Dashed lines are guides to the eye.

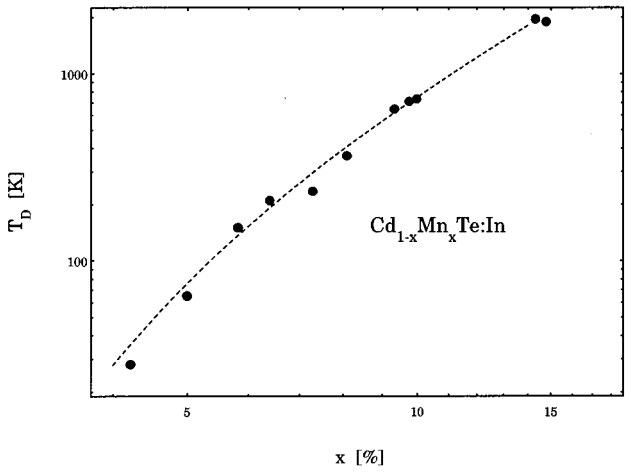

FIG. 3. The deep level activation temperature T_D $(=E_D/k_B)$ against Mn concentration x. Eleven samples of $Cd_{1-x}Mn_xTe$:In are plotted with Mn concentrations in the range 4% to 15%. The dashed line is a guide to the eye.

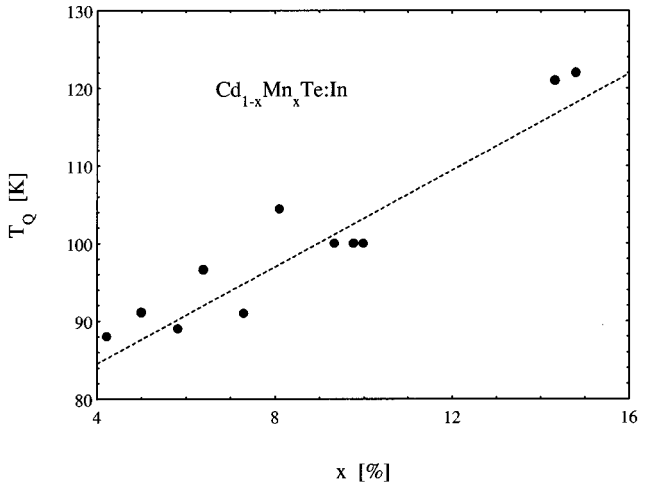

FIG. 4. PPC quenching temperature, T_Q, against Mn concentration, x. Eleven samples of $Cd_{1-x}Mn_xTe$:In are plotted with Mn concentrations in the range 4–15 %. The dashed line is a least squares fit to the data with $T_Q=3.11x+72.1$.

should see a change in n_c if one examines the behavior of the Bohr radius of the donor atom on going from $x=0-1.0$. As the electron effective mass and static dielectric constant are as yet unknown for zinc-blende MnTe, it is instructive to consider the case of $Cd_{1-x}Zn_xTe$. ZnTe has an electron effective mass of $m^*=0.16m_e$ and a static dielectric constant of $\varepsilon=9.2$; so we obtain a critical concentration $n_c\sim 6.3\times 10^{17}$ cm^{-3} from the Mott criterion. Thus we expect the critical concentration of $Cd_{1-x}Zn_xTe$ to be larger than the value for CdTe. This is in contrast to the work of Bennett *et al.*[12] where it was suggested that critical concentration of $Cd_{0.72}Zn_{0.28}Te$ was $n_c=4\times 10^{16}$ cm^{-3}, i.e., smaller than that of CdTe.

It is illuminating to examine the dependence of some of the transport properties in Table I on the Mn concentration, x. As might be expected there is a general trend of increasing resistivity with x at a constant temperature. There is a corresponding reduction in the room-temperature mobility with x, probably due to an increased alloy scattering rate. We also note that the infinite temperature extrapolation of the carrier density is roughly independent of x, up to our maximum value of 15%, showing that we are having no difficulty in producing n-type doping up to these Mn concentrations. Also, the increase in conductivity on illumination is seen to rise rather dramatically with x. This is because the increase in carrier concentration on illumination scales with the reduction in carrier concentration in cooling from high temperatures to 4.2 K, which is greater for more insulating samples, i.e., those with higher x. The most interesting quantities in terms of their x dependence are the ''deep level'' activation energy E_D (extracted from the transport data in the high-temperature region), and the PPC quenching temperature, T_Q. Figure 3 shows the deep level activation temperature $(T_D=E_D/k_B)$ as a function of the Mn concentration for eleven previously studied samples, including the four from set A, where a clear trend is observed. In Fig. 4 the PPC quenching temperature is plotted against x for these 11 samples. The quenching temperature is defined here as the temperature at which the dark resistivity curve joins the illuminated curve. As can be seen from Fig. 4 the quenching temperature has a roughly linear dependence on x for the range of Mn concentrations covered. These data elucidate the possibility of being able to estimate composition from transport measurements. However, a problem exists with the use of T_Q to predict x: the value of T_Q measured in any particular experiment is dependent on the rate at which the sample is warmed, with faster warming giving rise to a larger measured value of T_Q. The effect is shown in Fig. 5, where the measured T_Q value is plotted against the average warm up rate in the range 0.7 K min^{-1} to 10.5 K min^{-1}, for sample B5. These data are easily explained in terms of the temperature dependence of the relaxation rate of the PPC: consider Fig. 6, which plots normalized PPC against time for the same sample. Here it can be seen that at low temperatures the photoconductivity is truly persistent with no relaxation oc-

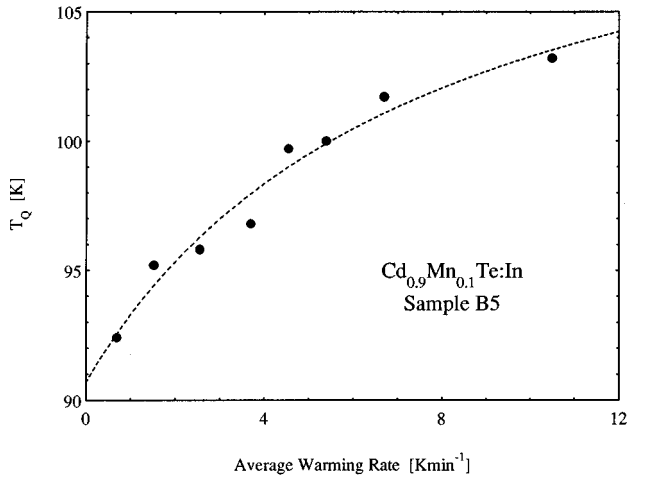

FIG. 5. Dependence of the quenching temperature T_Q on the average warm up rate, for sample B5. Here the sample is cooled to 40 K then warmed up at a certain rate, and the value of T_Q recorded. The dashed line is a guide to the eye.

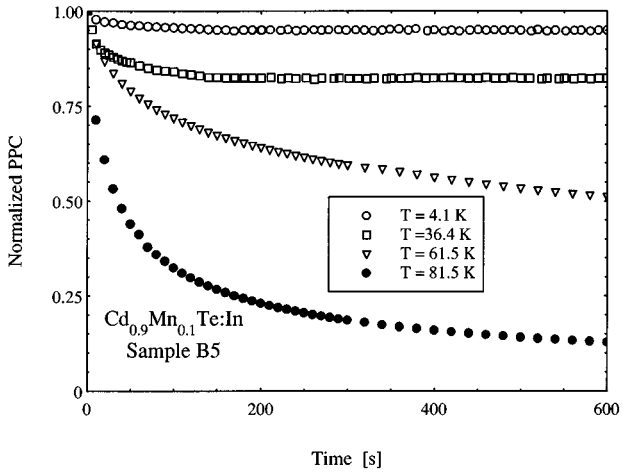

FIG. 6. Temperature dependence of the conductivity relaxation for sample B5. The relaxation is shown for four temperatures 4.1, 36.4, 61.5, and 81.5 K.

curring after about a minute. However, the higher-temperature curves show a significant relaxation of the photoconductivity on a much longer time scale, due to thermal excitation from a shallow effective-mass state to the deep level *DX* state. In fact, if the sample was kept at a constant temperature in this range, a situation would eventually be reached where the shallow state became exhausted of electrons, the conductivity being that of the dark level. Hence if the sample is warmed slowly, from the temperature at which it was illuminated, the quenching temperature will decrease.

Table II presents a summary of the phototransport data for sample set B. Samples B5, B6, B7, and B8 all show a similar behavior to set A with the exception that they are far more insulating. This is presumably due to a different level of compensation in these samples. As an example of this behavior, Fig. 7 shows the resistivity as a function of temperature for sample B5. The corresponding carrier concentration for this sample is shown in Fig. 8. The PPC is accompanied by an increase in the carrier concentration, with the PPC being quenched at a temperature of about 100 K. All samples in set

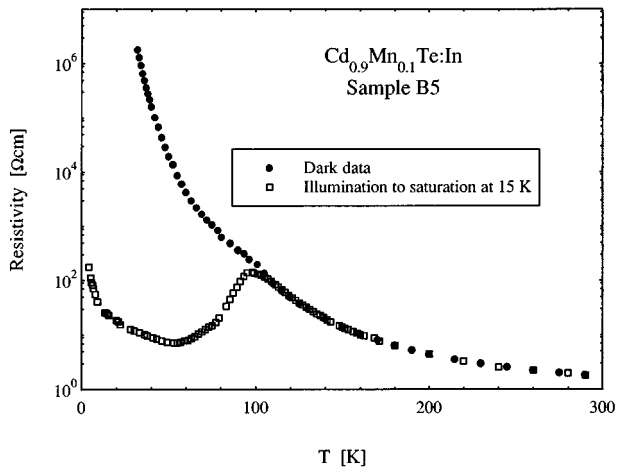

FIG. 7. Resistivity against temperature for sample B5 from room temperature to 4.2 K.

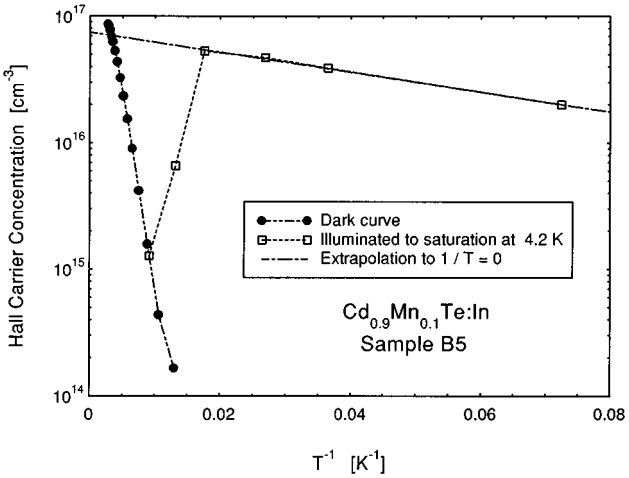

FIG. 8. Hall carrier concentration as a function of inverse temperature for sample B5, from 360 K down to 13.8 K. The data shown are for the dark case and for illumination to saturation at 4.2 K. The activation energy extracted from the illuminated curve is seen to be 1.56 meV. An extrapolation of the illuminated curve to infinite temperature gives $n = 7.8 \times 10^{16}$ cm^{-3}.

B show a similar behavior in terms of the dark carrier concentration and mobility. Figure 9 shows the mobility of sample B5 as an example. This clearly shows a crossover from the high-temperature region where phonon scattering is limiting the mobility to a regime below 200 K, where ionized impurity scattering dominates the mobility. A crossover at 200–250 K is seen in the mobility data for all of the samples. At lower temperatures (100 K and below) the mobility can fall to rather small values (<10 cm^2 V^{-1} s^{-1}) suggesting that the conductivity will proceed via a hopping mechanism. The illuminated mobility is greater than in the dark, as is normally the case.[1]

Sample B4 exhibits a very different behavior, with the PPC being supported up to higher temperatures. The resistivity and Hall carrier concentration for sample B4 are plotted in Fig. 10 as a function of temperature from 300 K down

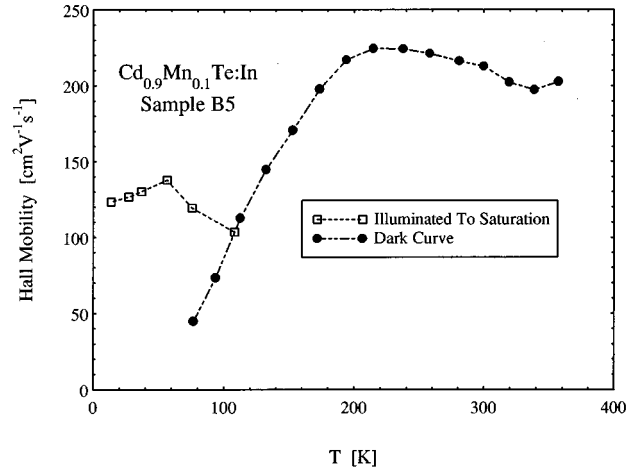

FIG. 9. Hall mobility against temperature for sample B5 from 360 K down to 13.8 K.

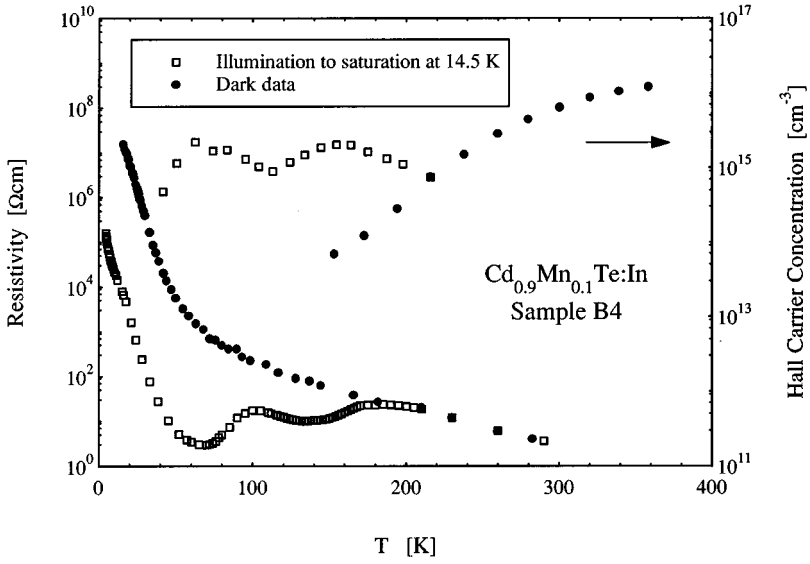

FIG. 10. Resistivity and Hall carrier concentration as a function of temperature for sample B4. A second stable PPC state is seen, with a quenching temperature of 190 K.

to 14.5 K. On cooling in the dark perfectly normal behavior is observed with the resistivity becoming unmeasurably large at ~20 K. The sample was illuminated at 14.5 K and then warmed slowly. Normal behavior is seen up to about 100 K, at which point the resistivity begins to fall again rather than increasing to join the dark curve. The resistivity eventually rises and joins the dark curve at 190 K (the average warming rate in this case was ~4 K $\min^{-1}$). As can been seen from this figure the increase in conductivity above 100 K is accompanied by a corresponding increase in the free-carrier concentration. To ensure that this effect is truly persistent photoconductivity the sample was cooled to various temperatures, illuminated, and the relaxation curves measured. This data is summarized in Fig. 11, where the % drop in conductance between 100 and 200 s is plotted against temperature. At low temperatures the photoconductivity is truly persistent, but as the sample is warmed the photoconductivity begins to relax, just as for sample B5. However, at about 120 K the photoconductivity becomes persistent again, with no relaxation taking place after about 100 s. Further warming induces relaxation of the photoconductivity as expected. Clearly the increase in conductivity and Hall carrier concentration are due to PPC. This sample is one of a small number which has been found to display this effect and constitutes the first observation of ''high-temperature PPC'' in $Cd_{1-x}Mn_xTe$:In. It should be noted that the samples displaying this effect are grown under nominally the same conditions as others which show no such behavior.

There are a number of possible origins of the second quenching temperature of the PPC in sample B4. It is recalled that Thio *et al.*[10] attributed the high quenching temperature PPC in $Cd_{0.72}Zn_{0.28}Te$:Cl to the multiple *DX* centers that Park and Chadi[11] have predicted to exist in CdTe, ZnTe, and $Cd_{1-x}Zn_xTe$ when doped with group-VII donors. However, the Park-Chadi model also predicts that group-III donors such as indium only exist in one *DX*-like state. Thus, either the high-temperature PPC observed in sample B4 has some other origin unconnected to the *DX* nature of the indium donor, or there may be a limit to applicability of the Park-Chadi theory to other CdTe-based II-VI alloys. Resolving this uncertainty is complicated by the fact that multiple *DX* centers with slightly different binding energies can arise because of the sensitivity of the impurity center to its local atomic environment.[20–23] Group IV donors in $Al_xGa_{1-x}As$ display a splitting of their ground state in the *DX* center configuration due to different possible numbers of Al neighbors. So the actual binding energy of the *DX* center should be labeled E^i_{DXn}, where $i=0,1,2,3$ is the number of Al atoms surrounding the donor in the *DX* center configuration, and *n* labels the type of *DX* center as evinced by the calculations of Park and Chadi. This local environment effect has been demonstrated by Mooney, Theis, and Calleja[23] when measuring the deep level transient spectroscopy (DLTS) spectra of Si-doped GaAs and $Al_xGa_{1-x}As$ samples: for the case of GaAs a single peak is found whereas three peaks appear for $Al_xGa_{1-x}As$. In addition to this Contrereas *et al.*[21] obtained electrical transport data which appear to confirm the conclusion that a number of *DX* states are apparent. It is worth noting that this effect is not confined to Si in $Al_xGa_{1-x}As$. Sallese *et al.*[22] have observed that the Te related *DX* center

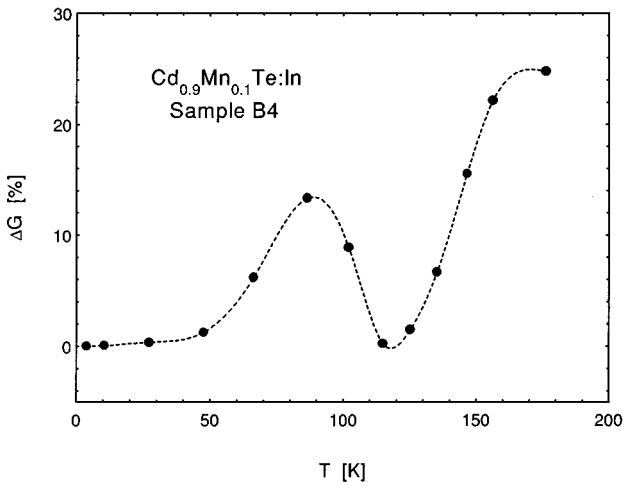

FIG. 11. Percentage drop in conductance on the relaxation curve between 100 and 200 seconds (ΔG) against temperature, for sample B4.

is also very sensitive to the local environment. However, Dobaczewski *et al.*[24] have demonstrated that multiple peaks in the DLTS spectra of $Al_{1-x}Ga_xAs$ are only observable in low quality or highly doped samples grown by molecular-beam epitaxy, and that any true alloy splitting is hidden in the broad DLTS peak observed in high quality samples. It is also suggested that such a structure in transport measurements will only be observed in low quality or heavily doped samples. Thus it is necessary to obtain information on the quality of the crystals when attempting to understand the origin of the high-temperature PPC in $Cd_{1-x}Mn_xTe$:In.

It is instructive to attempt to estimate what fraction of the In donor atoms will form a *DX* center with 0-, 1-, 2-, or 3-Mn atoms in the configuration. Very simply, if one considers a crystal with a certain number of indium atoms, then a number N_{DX} *DX* centers will form. Hence there are $4N_{DX}$ atoms of Cd or Mn in the *DX* center configurations. For a crystal with a Mn concentration x, the number of these atoms which are Mn is $4xN_{DX}$. Hence the average number of Mn atoms in a particular *DX* center is $4x$. So for $x=0.1$, as for sample B4, we obtain an average of 0.4-Mn atoms per center. In addition to this, a further simple calculation can be performed to estimate the probability of finding i Mn atoms in a *DX* center configuration given that a fraction x of them are Mn. If one assumes a simple statistical model with no clustering of Mn occurring, then for $x=0.1$ one obtains the probability of finding a center with $i=0$, 1, 2, or 3 Mn atoms as 66%, 30%, 3%, and 0.3%, respectively. If our data is to be explained on the basis of sensitivity to the local atomic environment then this might explain why only two stable PPC states are observed: the fraction of $i=2,3$ states present is rather small. It should also be noted that for the case of $Al_xGa_{1-x}As$:Si, material with $x>0.22$ is usually used in PPC studies, as this is the value of x below which the *DX* level is resonant with the conduction band. This leads to probabilities of 36.4%, 42.7%, 11.8%, and 3.06%, i.e., it is much more likely that the other *DX* configurations will be evident.

A source of PPC that is unrelated to the *DX* center has been proposed by Queisser and Theodoru.[25] Here photoexcited electrons are hindered in their attempts to recombine with holes by macroscopic barriers rather than the microscopic barriers presented by *DX* centers. This has been invoked to explain the existence of PPC in well defined heterostructural samples where the junctions provide the macroscopic barrier. A similar idea was proposed to explain the PPC in $Zn_{0.3}Cd_{0.7}Se$,[26,27] with random local potential fluctuations arising from compositional variations (producing variations in the conduction-band minima) being responsible for the PPC. However, the theoretical work of Shik and his co-workers[28] on persistent photoconductivity in inhomogeneous media concludes that such a mechanism on its own is unlikely to lead to this PPC, and it is, rather, the existence of a high level of compensating centers (e.g., cadmium vacancies) that lead to large conduction and valence-band edge modulation that is appropriate for long relaxation times of photocurrent. Thus once again we need to obtain information on the quality of the semiconducting material to determine whether such a mechanism for PPC is applicable to sample B4. It should be noted that this type of PPC results in a very different kind of relaxation to the conventional *DX* center PPC. After the removal of the illumination the conductivity is seen to relax appreciably over long periods of time (hundreds of seconds), whereas with the PPC supported by *DX* centers the low-temperature relaxation is small and rapid. The relaxation shown in Fig. 6 is typical of the samples of $Cd_{1-x}Mn_xTe$:In examined here. When considering the potential effects of compositional and compensational fluctuations on the PPC properties of $Cd_{1-x}Mn_xTe$:In it is important to consider the wavelength at which one is illuminating. In our case the illumination occurs at 1.3 eV which is considerably less than the band gap of the material, which is 1.7.5 eV for $x=0.1$. Hence, band-to-band transitions, which could lead to large relaxation times in the existence of fluctuations, should be negligible. Even with fluctuations in the conduction-band edge the minimum possible energy gap which can occur at any point is the CdTe band gap, i.e., 1.5 eV.

In addition to the electrical transport data, EDAX measurements were done on all of the samples. This technique produces a reasonable estimate of the Mn concentration to be made to within about 0.5%. More importantly it allows measurement of the level of compositional fluctuations within a particular sample. In addition to these measurements, the composition of one of the samples in set A was determined from mass spectroscopy, as indicated in Table I. These compositional fluctuations were measured in sample B4. Here, EDAX measurements are made every 10 μm along a line on the sample surface. The data show no large compositional fluctuation, with 20 such points producing a standard deviation of 0.61% Mn. In addition to this data, the composition of the crystal was measured in six different adjacent regions of area $100\mu\times100\,\mu\text{m}$.[2] This yields values for the Mn concentration of 0.107, 0.097, 0.095, 0.100, 0.900, and 0.900, again no significant spatial variation of the composition is found. This leads us to the conclusion that the level of compositional fluctuations within the samples showing the anomalous PPC behavior is insignificant. Indeed the measured fluctuations in the other samples, with normal PPC quenching temperatures, are of a similar level.

As well as the above-mentioned explanations of our data there is also the rather simple explanation that there are regions of very large x material which will produce a *DX* center with a much larger binding energy, and hence quenching temperature. It is interesting to attempt to estimate the manganese concentration required to bring about a quenching temperature of the order of 190 K. If we were to use our measured dependence of the quenching temperature on x and extrapolate to 190 K, we arrive at an x value of 0.38. Although this involves extrapolation well beyond the range of composition measured in this study, it is clear that a very large value of x will result. It is difficult to imagine how a crystal which is nominally 10% could have such large x regions within it, and indeed no such regions were detected by the EDAX measurements.

V. SUMMARY AND CONCLUSIONS

In summary, we have investigated the PPC effect in several samples of $Cd_{1-x}Mn_xTe$:In. We have concluded that some of these samples are rather close to the MIT. Photodoping or the application of a magnetic field could well induce a transition. Further work at lower temperatures will be re-

quired to ascertain whether such a phase transition takes place. The compositional dependence of the phototransport parameters has also been investigated, showing that they could be used to estimate composition. In particular the quenching temperature of the PPC lends itself well to such applications as it has linear dependence on the manganese concentration, x in $Cd_{1-x}Mn_xTe$:In, the only problem being the dependence of T_Q on the warming rate. This could be applicable to other persistently photoconducting alloys such as $Al_xGa_{1-x}As$. We have also discovered a sample which exhibits PPC at elevated temperatures. This sample supports PPC up to 190 K compared to a typical value of approximately 100 K for a 10% Mn sample. Such samples are extremely interesting as it has already been pointed out that a material which supports PPC at room temperature will have an enormous application potential. The writing of erasable, conductive patterns on an insulating background (which has already been successfully achieved in $Al_xGa_{1-x}As$ and $Cd_{1-x}Zn_xTe$) is the basis of these potential applications such as optical switching, holography, data storage, etc. The other major requirement for such applications would be a high level of metallicity. The work mentioned above on the metal-insulator transition appears rather relevant. In addition, there are several reasons why a II-VI semiconductor such as $Cd_{1-x}Mn_xTe$:In is advantageous—their ease of growth in bulk form for instance. In particular, it has been suggested that DX center binding energies show promise of being much larger in II-VI semiconductors than in III-V's. This would lead to PPC at higher temperatures, if indeed the elevated temperature PPC in this material is due to DX center formation. This leads us to our conclusions with regard to the cause of the high-temperature PPC effects.

Of the various models reviewed in the introduction the easiest to eliminate are the ones based on the existence of regions of high manganese concentration or fluctuations in the Mn concentration. This was the motivation for the EDAX measurements presented earlier, which indicate no large compositional fluctuations. In addition to this evidence, we must also consider the relevance of the work by Shik,[28] which indicates that compositional fluctuations alone cannot account for long relaxation times and PPC: fluctuations in compensation are required to produce PPC.

We have considered the effect of these compensational fluctuations and have shown that it is possible that they make a small contribution to the PPC in our samples. Perhaps the most important point to make however, is that even if these fluctuations are of importance, they cannot fully explain our data in that they cannot be responsible for a second stable state in the PPC—they can only enhance the existing effect. This is in contrast to the explanations based on multiple DX centers. We have also shown that as our excitation energy is smaller than the energy gap regardless of the size of the fluctuations, the photoconductivity due to band-to-band transitions should be negligible.

It seems therefore that an explanation based on the existence of multiple DX centers in $Cd_{1-x}Mn_xTe$:In is the only plausible one. Although this is in disagreement with the theoretical predictions of Park and Chadi,[11] the apparent conflict between experiment and theory could be reconciled if the effects of the local environment prove to be important. If this were the case, then the elevated temperature PPC effect could be due to a shift in the energetic position of the In DX center caused by DX configurations with differing numbers of Mn atoms, rather than the existence of another DX center with a slightly different atomic configuration to the original ''broken bond'' DX like state. In other words, we are observing a number of states E^i_{DXn}, where $i=0,1,2,3$ is the number of Mn atoms clustered around the donor atom. Simple calculations which estimate the probability of the occurrence of DX center configurations with i Mn atoms could explain why only two stable states are observed in the transport data. Another possibility of course, is that, as mentioned earlier, the calculations of Park and Chadi are not strictly applicable to $Cd_{1-x}Mn_xTe$:In, leaving no such restriction on the number of DX configurations possible for In as a donor in $Cd_{1-x}Mn_xTe$:In. Further theoretical work in this area would certainly be of benefit in determining the mechanism for this elevated temperature PPC effect. Although it seems likely that the second stable PPC state we observe is due to a second DX center, it is difficult to ascertain by which of the mechanisms detailed above it is created.

In conclusion we have observed elevated temperature PPC in $Cd_{1-x}Mn_xTe$:In. PPC would have an enormous application potential if the requirements of room-temperature operation and high metallicity in illuminated regions could be realized. Given this, $Cd_{1-x}Mn_xTe$:In appears to be a possible candidate for this kind of application. We have attempted to identify the mechanism for the elevated temperature PPC effect by considering several possibilities. Whether the PPC is due to DX centers with different configurations, or to the effects of the local atomic environment on the DX center energy, cannot be resolved as yet. It is clear, however, that the elevated temperature PPC is due to some form of multiple DX centers.

[1] I. Terry, T. Penney, S. von Molnar, J. M. Rigotty, and P. Becla, Solid State Commun. **84**, 235 (1992); N. G. Semaltianos, G. Karczewski, T. Wojtowicz, and J. K. Furdyna, Phys. Rev. B **47**, 12 540 (1993).

[2] B. C. Burkey, R. P. Khosla, J. R. Fischer, and D. L. Losee, J. Appl. Phys. **147**, 1095 (1976).

[3] K. Khatchaturyan, M. Kaminska, E. R. Weber, P. Becla, and R. A. Street, Phys. Rev. B **40**, 6304 (1989).

[4] G. W. Iseler, J. A. Kaflas, A. J. Strauss, H. F. MacMillan, and R. H. Bube, Solid State Commun. **10**, 619 (1972).

[5] For a recent review see P. M. Mooney, J. Appl. Phys. **67**, 3 (1990).

[6] D. J. Chadi and K. J. Chang, Phys. Rev. Lett. **61**, 873 (1988).

[7] D. J. Chadi and K. J. Chang, Phys. Rev. B **39**, 10 063 (1989).

[8] T. Thio, R. A. Linke, G. E. Devlin, J. W. Bennett, D. J. Chadi, and M. Mizuta, Appl. Phys. Lett. **65**, 1802 (1994).

[9] R. A. Linke, T. Thio, D. J. Chadi, and G. E. Devlin, Appl. Phys. Lett. **65**, 16 (1994).

[10] T. Thio, J. W. Bennett, D. J. Chadi, R. A. Linke, and P. Becla, J. Cryst. Growth **159**, 345 (1996).

[11] C. H. Park and D. J. Chadi, Phys. Rev. B **52**, 11 884 (1995).
[12] J. W. Bennett, T. Thio, S. E. Kabakoff, D. J. Chadi, R. A. Linke, and P. Becla, J. Appl. Phys. **78**, 5827 (1995).
[13] S. Katsumoto, in *Anderson Localization*, edited by T. Ando and H. Fukuyama (Springer-Verlag, Berlin, 1987), p. 45.
[14] N. F. Mott, *Conduction in Non-Crystalline Materials* (Oxford Clarendon, Oxford, 1987).
[15] T. Wojtowicz, T. Deitl, M. Sawicki, W. Plesiewicz, and J. Jaroszynski, Phys. Rev. Lett. **56**, 2419 (1986).
[16] S. von Molnar and T. Penny, in *Localization and Metal-Insulator Transitions*, edited by H. Fritzche and D. Adler (Plenum, New York, 1985), p. 183.
[17] Y. Shapira, N. F. Oliveira, Jr., P. Becla, and T. Q. Vu, Phys. Rev. B **41** 5931 (1990).
[18] Y. Shapira, N. F. Oliveira, Jr., D. H. Ridgley, R. Kershaw, K. Dwight, and A. Wold, Phys. Rev. B **34**, 4187 (1986).
[19] H. C. Casey, Jr. and M. B. Panich, *Heterostructure Lasers* (Academic, London, 1978), p. 194.
[20] E. Calleja, F. Garcia, A. Gomez, E. Munoz, P. M. Monney, T. N. Morgan, and S. L. Wright, Appl. Phys. Lett. **56**, 934 (1990).
[21] S. Contrereas, V. Mosser, R. Piotrzkowski, P. Lorenzin, J. Sicart, P. Jeanjean, J. L. Robert, and W. Zawadzki, Semicond. Sci. Technol. **6**, B58 (1991).
[22] J. M. Sallese, D. K. Maude, M. L. Fille, U. Willke, P. Gibart, and J. C. Portal, Semicond. Sci. Technol. **7**, 1245 (1992).
[23] P. M. Mooney, T. N. Theis, and E. Calleja, J. Electron. Mater. **20**, 23 (1991).
[24] L. Dobaczewski, P. Kaczor, M. Missous, A. R. Peaker, and Z. R. Zytkiewicz, J. Appl. Phys. **78**, 2468 (1995).
[25] H. J. Queisser and D. E. Theodoru, Phys. Rev. B **33**, 4027 (1986).
[26] J. Y. Lin and H. X. Jiang, Phys. Rev. B **41**, 5178 (1990).
[27] H. X. Jiang and J. Y. Lin, Phys. Rev. Lett. **64**, 2547 (1990).
[28] A. Ya. Shik, Zh. Éksp. Teor. Fiz. **68**, 1859 (1975) [Sov. Phys. JETP **41**, 932 (1976)].